PHYSICAL REVIEW B **72**, 241309(R) (2005)

Hole spin anisotropy in single Mn-doped quantum dots

Y. Léger,* L. Besombes, L. Maingault, D. Ferrand, and H. Mariette
CEA-CNRS group "Nanophysique et Semiconducteurs," Laboratoire de Spectrométrie Physique, CNRS and Université Joseph Fourier-Grenoble 1, BP 87, F-38402 St Martin d'Hères, France
(Received 27 July 2005; revised manuscript received 6 October 2005; published 15 December 2005)

The anisotropy in the exchange interaction between a single magnetic atom and a single exciton confined in a quantum dot (QD) is revealed experimentally. In a transverse magnetic field we directly observe the orientation of the magnetic ion spin along the resultant direction of the external magnetic field and the hole exchange field. With an increasing transverse magnetic field, this orientation progressively cancels the exchange interaction with the hole and at a high field the fine structure is mainly controlled by the electron-Mn coupling. At intermediate fields, we observe emission replicas caused by multiple spin flips within the Zeeman split ground state of a single Mn. All these features are well modeled by the magnetic field dependence of the stationary states of a single Mn spin in the exchange field of a heavy-hole exciton.

DOI: 10.1103/PhysRevB.72.241309 PACS number(s): 78.67.Hc, 78.55.Et, 75.75.+a

The control of the interaction between individual spin-polarized carriers and isolated magnetic atoms is of fundamental interest to understand the mechanism involved in spin transfer in magnetic materials. Spin transfer could lead to the development of spintronic devices in which the spin state of magnetic atoms is controlled by the injection of a spin-polarized current and not by an external magnetic field, such as in conventional magnetic memories.[1] With the development of nanostructures such as diluted magnetic semiconductor quantum dots (QDs), the control of spin-related phenomena on a nanoscale becomes possible.[2–4] However, the spin properties of these systems are dominated by statistical magnetic fluctuations. This limit has been recently overcome by studying the interaction between a few confined carriers and a *single* magnetic atom.[5–8]. Such a system, based on II-VI self-assembled QDs doped with Mn atoms, allows us to analyze, in a solid state environment, the interaction between single carriers (electron or hole) and an individual magnetic atom.

In this paper, we analyze the influence of the hole-spin anisotropy on the magneto-optical properties of the exciton-manganese (*X*-Mn) system. Up to now, the effects of this anisotropy on *X*-Mn coupling have only been considered in collective phenomena such as the formation of magnetic polaron involving individual carriers and a large number of magnetic atoms.[9,10] Here, the observation of the spin state of a single Mn atom interacting with a single exciton in a transverse magnetic field allows us to monitor the orientation of the Mn spin in the exchange field of the hole. This progressive orientation is responsible (i) for the decrease of the overall splitting of the *X*-Mn structure and (ii) for the appearance of optical recombination occurring with multiple spin flips within the Zeeman split ground state of the Mn. This transverse magnetic field dependence is well modeled by the evolution of the stationary states of a single Mn spin in the exchange field of a heavy-hole exciton. For some Mn-doped QDs, an influence of the valence band mixing can be identified in the zero magnetic field spectra. In these cases, a non-negligible contribution of the hole-Mn interaction remains even at high a transverse magnetic field.

Microspectroscopy is used to study the magneto-optical properties of self-assembled CdTe/ZnTe QDs doped with single Mn atoms. A low density of Mn atoms is introduced in the QD plane exploiting the Mn intermixing through a ZnTe spacer layer grown on a ZnMnTe barrier.[5,11] The low temperature (5 K) photoluminescence (PL) of single QDs is excited with the 514.5 nm line of an argon laser and collected through aluminum shadow masks with 0.2–1.0 μm apertures. The PL is then dispersed by a 2 m double monochromator and detected by a nitrogen-cooled Si charged-coupled device.

Figure 1 shows the experimental and calculated spectra for two different Mn-doped QDs (QD1 and QD2) at a zero magnetic field. QD1 emission is composed of six lines roughly equally spaced in energy. This emission structure has been described in details in Refs. 5 and 7. The isotropic *e*-Mn exchange interaction can be described by an Heisenberg Hamiltonian. In the pure heavy hole approximation, the *h*-Mn exchange interaction is reduced to the Ising term. This

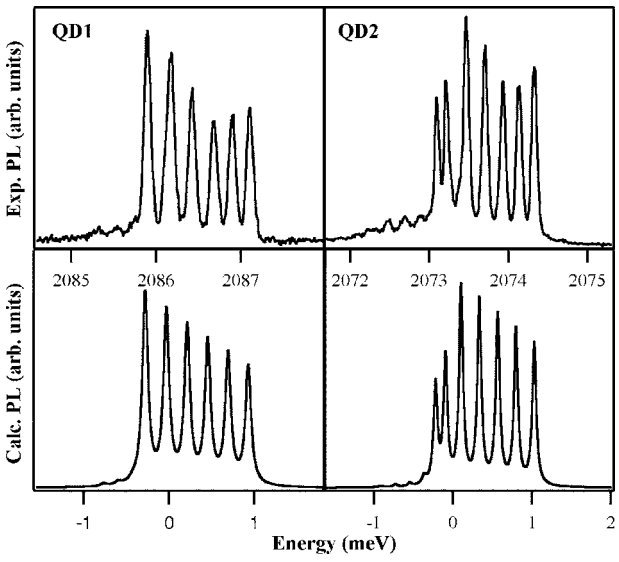

FIG. 1. Experimental and calculated spectra at a zero magnetic field for two QDs. QD1 is a dot where there is no experimental evidence of valence band mixing. For QD2, the appearance of dark states at a zero magnetic field is an evidence of valence band mixing.

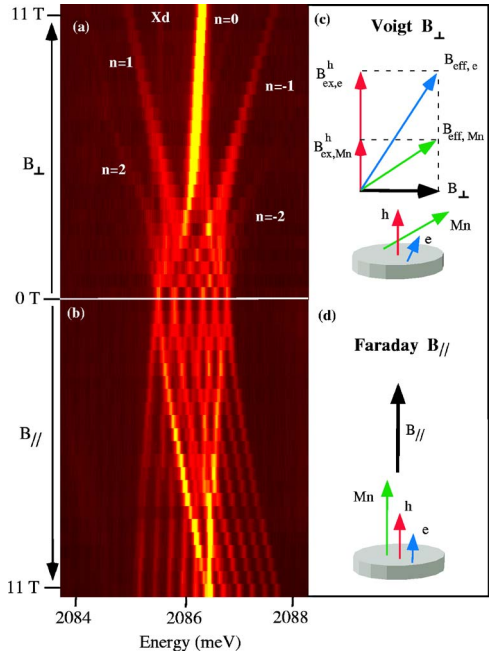

FIG. 2. (Color online) (a) and (b) are contour plots presenting the magnetic field dependence of QD1 emission structure. (a) Voigt configuration, (b) Faraday configuration (yellow or light gray: high intensity; red or dark gray: low intensity). (c) and (d) are schemes of the spin orientations of the electron (blue), the hole (red), and the Mn atom (green) in Voigt and in Faraday configurations, respectively.

interaction imposes the quantization axis along the growth axis and lifts the degeneracy of the six Mn spin projections: The exchange interaction of the charge carriers and electrons from the d shell of the Mn atom is then described by the Hamiltonian,

$$H_{\mathrm{ex}} = I_e\left[\sigma_z S_z + \tfrac{1}{2}(\sigma_- S_+ + \sigma_+ S_-)\right] + I_{\mathrm{h}} j_z S_z, \qquad (1)$$

where $I_{e(h)}$ is the e-Mn (h-Mn) exchange integral and σ, j, and S are the electron, hole, and Mn spin operators respectively ($S=5/2$).

By contrast, QD2 presents a more complex structure with seven main emission lines and some additional weak intensity lines on the low energy side of the spectra. These features can only be explained by considering a valence band mixing that couples bright and dark exciton states. In a first approximation the valence band mixing couples $|\pm 3/2\rangle$ heavy holes with $|\mp 1/2\rangle$ light holes allowing simultaneous spin-flips between hole and Mn atom.[12–14] This effect can be described by introducing in the Hamiltonian (1) a perturbative term $\epsilon I_h(\tilde{j}_- S_+ + \tilde{j}_+ S_-)$. Here, the efficiency of the valence band mixing appears through an adjustable parameter ϵ. The pseudospin operator $\tilde{j}_\pm$ flips the hole from $\mp 3/2$ to $\pm 3/2$. The characteristic emission structure of QD2 can be well described taking into account this perturbation (see Fig. 1).

The anisotropy of the exchange interaction in a Mn-doped QD is directly revealed when comparing the magnetic field dependence of the emission in Faraday and Voigt configurations. These are presented in Figs. 2(a) and 2(b) for QD1.

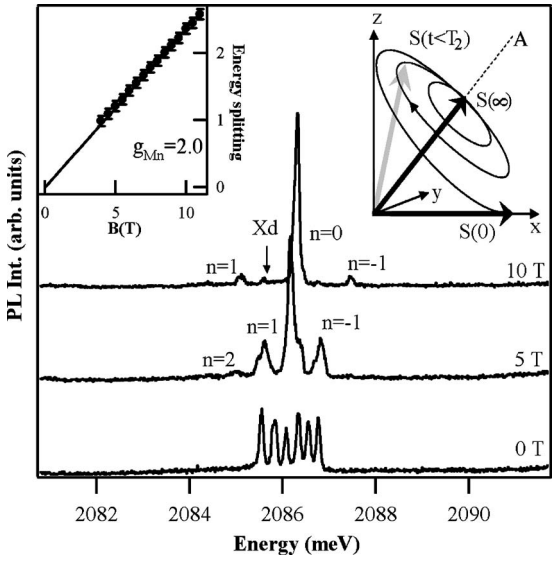

FIG. 3. PL spectra of QD1 under magnetic field in Voigt geometry. The left inset presents the magnetic field dependence of the energy splitting between the emission replicas $n=1$ and $n=-1$. This linear evolution corresponds to a Mn g factor $g_{Mn}=2.0$. The right inset is an illustration of the precession motion of S in $B_{eff}=B_{ext}+B^h_{ex,Mn}$.

The magneto-optic behavior in a Faraday configuration (magnetic field applied along the growth axis z) has already been studied in details in Ref. 5. Under a longitudinal magnetic field ($B_{ext}\|z$), the quantization axis along the growth direction is conserved [see Fig. 2(d)]. The ground state (Mn atom) splits into six levels and each level of the exciton-Mn system splits with the Zeeman energy of the exciton and shifts in energy due to the Zeeman effect of the Mn atom. As the initial and final states are quantified along the same axis, the Mn spin projection is conserved during the optical transition and there is no influence of the Mn Zeeman energy on the emission spectrum. Only the exciton Zeeman splitting is observed for each of the six zero field lines leading to the typical magnetic dependence observed in Fig. 2(b).

The magnetic field dependence in a Voigt configuration [Fig. 2(a)] is totally different, revealing the anisotropy of the magneto-optic response of the system. When increasing the transverse magnetic field ($B_{ext}\|x$), each of the six lines splits in a large fan. Many lines appear, crossing and then joining in different sets. Five sets can clearly be observed: a central one that progressively takes all the intensity and four replicas which linearly shift with B_{ext}. The intensity of the replicas is very weak compared to the central line and decreases with the increase of B_{ext}. The energy spacing between these sets corresponds to an integer number n of the Zeeman energy of the Mn atom ($g_{Mn}\mu_B B_{ext}$). The linear shift of the replicas is well reproduced with a Mn g factor $g_{Mn}=2.0$ (left inset of Fig. 3). At a high transverse field, an additional emission line (X_d) appears about 0.7 meV below the central set (Fig. 3). Its intensity increases with increasing the magnetic field and its energy follows the central set. Finally, the overall splitting of each line set decreases progressively when increasing B_{ext}. This effect is particularly clear for the central group of emission lines.

This complex magneto-optic behavior can be qualitatively explained by considering the precession motion of a single Mn spin in external and exchange fields. Let us first consider the demonstrative extreme case of a pure heavy hole exciton interacting with the Mn ion. It is convenient to introduce the two effective exchange fields induced by the electron ($B^e_{ex,Mn}=I_e\sigma/g_{Mn}\mu_B$) and the hole ($B^h_{ex,Mn}=I_h j/g_{Mn}\mu_B$). In this framework, the spin Hamiltonian (1) can be rewritten as $g_{Mn}\mu_B[(B^e_{ex,Mn}+B^h_{ex,Mn}+B_{ext})S]$ where we can define a resulting effective magnetic field acting on the Mn spin $B_{eff}=B^e_{ex,Mn}+B^h_{ex,Mn}+B_{ext}$. Typical values of these exchange fields for the studied QDs are $B^e_{ex,Mn}\approx 0.3T$ and $B^h_{ex,Mn}\approx 1.8T$.

Such exchange fields can also be defined to describe the electron behavior. The *e*-Mn and the *e*-*h* exchange interactions are equivalent to effective magnetic fields $B^{Mn}_{ex,e}\simeq 3T$ and $B^h_{ex,e}\simeq 11T$ respectively. The *e*-Mn exchange interaction is small compared to the other exchange energies and in the following, we will neglect its influence on the spin orientation of the particles (electron and Mn). In this way, we can easily define the total effective magnetic fields for the electron and for the Mn spin [see Fig. 2(c)]. Whereas the heavy-hole spin is blocked along the growth axis, the electron and the Mn spins rotate about **y** when an external in-plane magnetic field B_{ext} is applied along the **x** axis.

The orientation of the Mn spin is the key point in the understanding of the Voigt magneto-optic behavior. Under an external magnetic field in Voigt geometry ($B_{ext}\|x$), the Mn spin is oriented along **x**. After the creation of a confined exciton, the Mn spin is rotated away from the **x** axis by the strong exchange field of the hole $B^h_{ex,Mn}\|z$ and begins to precess with Larmor frequency around the resulting effective field $B_{eff}=B_{ext}+B^h_{ex,Mn}$ (the right inset of Fig. 3).[15] The component of $S(t)$ transversal to the field B_{eff} relaxes within the time T_2 which corresponds to the dephasing time of the coherent precession of the magnetic ion spin. The *X*-Mn complex will then further relax its energy within the time T_1. Under nonresonant excitation, because of the spin-spin coupling with the created carriers, T_1 is found to be shorter than the exciton lifetime τ[5]. After T_1, the *X*-Mn complex reaches its stationary state with the Mn spin directed along the effective field B_{eff}. When the exciton recombines, after a delay τ, the projection of the Mn spin on B_{ext}, $S_x(\tau)$, differs from the initial value $S_x(0)=S(0)$.[15] The energy of the emitted light in the recombination process is modified by the energy spent (or win) to reorient the Mn spin, which is an integer number n of energy steps of a single spin flip. These spin flips are responsible for the replicas observed in the luminescence in Voigt geometry.

The probability of these spin flips depends on the change in the quantization axis direction during the recombination process. When an exciton is present in the QD we can define an effective quantization axis for the Mn spin, called *A* axis, orientated along the sum of external and exchange fields. During the recombination, the Mn spin has to pass from an eigenstate of $\mathbf{S}_A$ to an eigenstates of $\mathbf{S}_x$. This corresponds to the projection of a spin 5/2 [Fig. 4(c)]. The probability of transition from a given spin state along the *A* axis, noted S_A, to the S_x state is given by the 5/2 rotation matrix.[16] Every

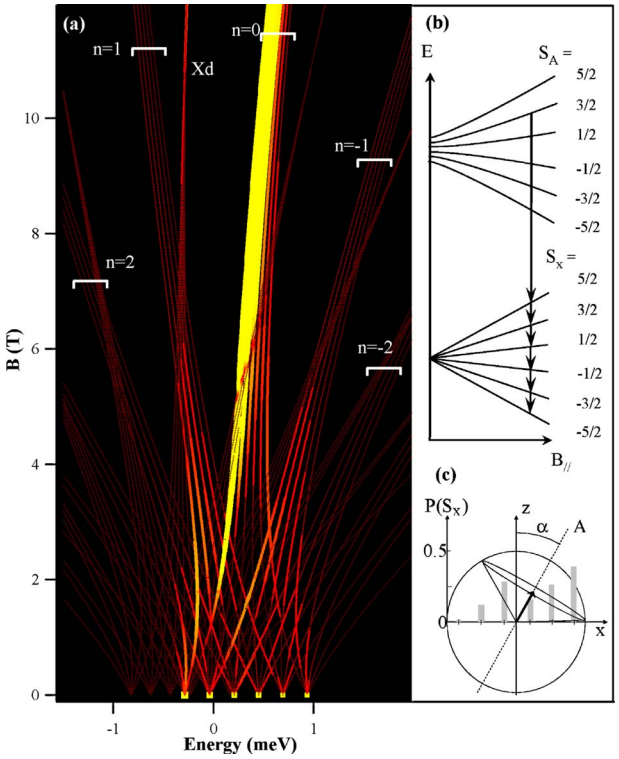

FIG. 4. (Color online) (a) Simulation of the magnetic field dependence of QD1 emission in a Voigt configuration. Under a high field, several sets of lines are observed, spaced by the Zeeman energy of the Mn atom. (b) Energy level diagram of the Mn-doped QD in a transverse magnetic field. The quantization axis in the initial state (*A*) differs from the quantization axis in the ground state (*x*). (c) Illustration of the rotation of a spin 5/2 with a projection $S_A=3/2$ by an angle $\pi/2-\alpha$ from an axis *A* to the *x* axis.

excitonic state associated with a given S_A Mn spin can recombine on any of the S_x final Mn spin states, except when the two quantization axes are identical. Considering the energy level diagram presented in Fig. 4(b), one notes that now the Mn Zeeman splitting influences the emission spectrum: Six optical transitions take place without any influence of the Mn Zeeman energy (conservation of the Mn spin projection), forming the $n=0$ set; five with a $g_{Mn}\mu_B B_{ext}$ shift (and five with $-g_{Mn}\mu_B B_{ext}$) forming $n=\pm 1$ sets; four with a $2g_{Mn}\mu_B B_{ext}$ shift, etc. Under a high transverse magnetic field ($B_{ext}\gg B^h_{ex,Mn}$), the initial and final quantization axes merge, the spin blockade is restored and only the transitions in which the Mn spin projection is conserved become possible. As observed in the experimental data, the replicas disappear.

The rotation of the Mn spin in the fixed exchange field of the hole progressively cancel the *h*-Mn exchange energy. Under a high transverse magnetic field, electron and Mn spins are both aligned with the **x** axis and only the *e*-Mn exchange remains. This orientation of the Mn spin explains the decrease of the *X*-Mn splitting clearly observed in the central set of emission lines. Moreover, as the electron spin rotates and tends to be aligned with the *x* axis, radiative and nonradiative excitons can no longer be defined. As in nonmagnetic QDs, under a transverse magnetic field, *dark* exciton states (note X_d in Fig. 3) progressively take some oscillator

strength and appear on the low energy side of the bright exciton structure.

A more quantitative model of the Voigt magneto-optic response was carried out. As the optical recombination occurs after a stationary state of the *X*-Mn system has been reached, a simulation of the emission structure can be obtained by diagonalizing the Hamiltonian of the *X*-Mn system in the subspace of a pure heavy-holes exciton. The obtained optical transitions are presented in Fig. 4(a). The *e*-Mn (I_e =50 μeV) and the *h*-Mn (I_h=−140 μeV) exchange interactions are extracted from the magneto-optic behavior in a Faraday configuration.[5] The *e*-*h* exchange integral (430 μeV) agrees well with previous work.[17] For the magnetic field dependence we choose a pure isotropic electron (g_e=−1) and Mn (g_{Mn}=2) *g* factors. The hole *g* factor is completely anisotropic with g_h^z=−0.1 and g_h^x=g_h^y=0. A diamagnetic factor γ=1.45 μeV/T^2 is also introduced. The initial and final eigenstates are calculated in the $\mathbf{S}_z$ basis. In order to obtain each transition intensity, we calculated the projection of the bright exciton part of each eigenstate of the *X*-Mn system on the final state (Mn in a transverse field). A thermal distribution in the excited states is also taken into account with an effective temperature of 30 K (which differs from the lattice temperature as explained in Ref. 5). There is a good agreement between the experimental data and this simple model. The main characteristics are well reproduced, namely the different sets of lines, their intensity evolution, the number of line within each set, and the appearance of the *dark* states at high magnetic fields.

The magnetic field evolution of the PL of QD2, in which an influence of the valence band mixing has been identified, presents the same characteristic features (see inset of Fig. 5). Nevertheless a difference between QD1 and QD2 appears in the overall splitting of the central set of lines. This splitting is roughly similar at a zero magnetic field for the two dots, but its decrease in a transverse field is less pronounced for QD1 than for QD2 (Fig. 5). Moreover, our pure heavy-hole model reproduces quite well a QD1 evolution but it is inadequate for a QD2. The valence band mixing already observed for QD2 in the zero magnetic field spectrum (Fig. 1) also induces a nonzero in-plane hole *g* factor and allows simultaneous hole-Mn spin flips. Both effects explain why it is not possible to completely cancel the hole-Mn exchange interaction even in a large transverse magnetic field.

In summary, we have shown the influence of the hole spin anisotropy on the exchange interaction between a single Mn atom and an individual confined exciton. In Voigt geometry, the orientation of the Mn spin along the sum of the external and hole exchange fields progressively cancels the *h*-Mn exchange interaction and allows optical transitions with Mn spin flips. The valence band mixing and thus the hole spin anisotropy vary strongly from dot to dot and a more accurate investigation of the valence band mixing effects on single Mn-doped QDs would be of great interest. However, for some dots, the heavy-hole approximation is justified. In these cases, the injection of a single exciton (or a hole) in a QD doped with a single magnetic atom acts as a pulse of magnetic field along the growth axis. This pulsed exchange field could be used to control the dynamics of a single magnetic atom embedded in a QD.

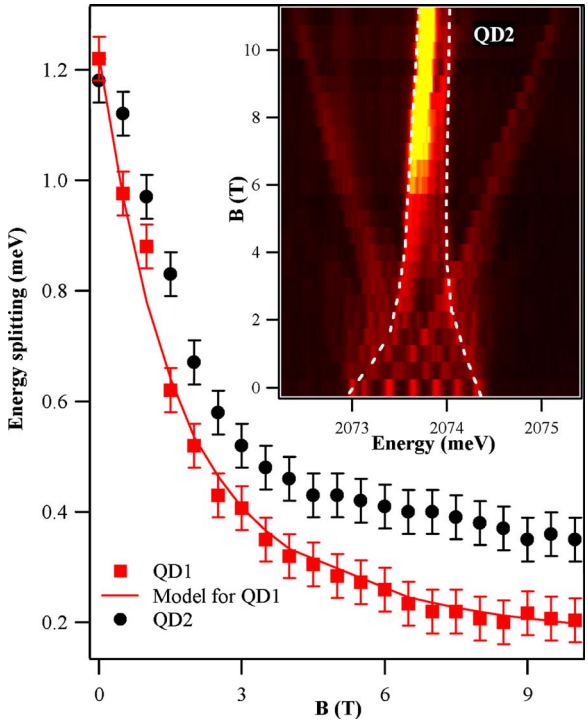

FIG. 5. (Color online) Transverse magnetic field dependence of the experimental *X*-Mn splittings for the central set of lines of QD1 and QD2. QD1 evolution can be well reproduced by the pure heavy-hole model. The inset shows the magnetic field dependence of QD2 emission in a Voigt configuration.

*Electronic address: yleger@spectro.ujf-grenoble.fr

[1] I. N. Krivorotov *et al.*, Science **307**, 228, (2005).
[2] S. A. Wolf *et al.*, Science **294**, 1488 (2001).
[3] G. Bacher *et al.*, Phys. Rev. Lett. **89**, 127201 (2002).
[4] A. Hundt *et al.*, Phys. Rev. B **69**, 121309(R) (2002).
[5] L. Besombes *et al.*, Phys. Rev. Lett. **93**, 207403 (2004).
[6] L. Besombes *et al.*, Phys. Rev. B **71**, 161307(R) (2005).
[7] A. O. Govorov and A. V. Kalameitsev, Phys. Rev. B **71**, 035338 (2005).
[8] Y. Léger *et al.*, Phys. Rev. Lett. **95**, 047403 (2005).
[9] P. S. Dorozhkin *et al.*, Phys. Rev. B **68**, 195313 (2003).
[10] J. Stuhler *et al.*, Phys. Rev. Lett. **74**, 2567 (1995).
[11] F. Tinjod *et al.*, Appl. Phys. Lett. **82**, 4340 (2003).
[12] F. V. Kyrychenko and J. Kossut, Phys. Rev. B **70**, 205317 (2004).
[13] J. Fernandez Rossier (unpublished).
[14] A. V. Koudinov *et al.*, Phys. Rev. B **70**, 241305(R) (2004).
[15] D. R. Yakovlev *et al.*, Phys. Rev. B **56**, 9782 (1997).
[16] R. N. Zare, *Angular Momentum* (Wiley, New York, 1988).
[17] L. Besombes *et al.*, Phys. Rev. Lett. **85**, 425 (2000).